MOLECULAR AND CELLULAR BIOLOGY, May 1995, p. 2663–2671 Vol. 15, No. 5
0270-7306/95/$04.00+0

Genetic Selection for Balanced Retroviral Splicing: Novel Regulation Involving the Second Step Can Be Mediated by Transitions in the Polypyrimidine Tract

JOHN BOUCK,[1,2] XIANG-DONG FU,[3] ANNA MARIE SKALKA,[1,2] AND RICHARD A. KATZ[1]*

Institute for Cancer Research, Fox Chase Cancer Center, Philadelphia, Pennsylvania 19111[1]; Division of Cellular and Molecular Medicine, University of California at San Diego, La Jolla, California 92093-0651[3]; and Molecular Biology Graduate Group, University of Pennsylvania, Philadelphia, Pennsylvania 19104[2]

Received 8 December 1994/Returned for modification 1 February 1995/Accepted 2 March 1995

Incomplete splicing is essential for retroviral replication; and in simple retroviruses, splicing regulation appears to occur entirely in *cis*. Our previous studies, using avian sarcoma virus, indicated that weak splicing signals allow transcripts to escape the splicing pathway. We also isolated a series of avian sarcoma virus mutants in which *env* mRNA splicing was regulated by mechanisms distinct from those of the wild-type virus. In vitro splicing experiments with one such mutant (insertion suppressor 1 [IS1]) revealed that exon 1 and lariat-exon 2 intermediates were produced (step 1) but the exons were not efficiently ligated (step 2). In this work, we have studied the mechanism of this second-step block as well as its biological relevance. Our results show that the second-step block can be overcome by extending the polypyrimidine tract, and this causes an oversplicing defect in vivo. The requirement for regulated splicing was exploited to isolate new suppressor mutations that restored viral growth by down-regulating splicing. One suppressor consisted of a single U-to-C transition in the polypyrimidine tract; a second included this same change as well as an additional U-to-C transition within a uridine stretch in the polypyrimidine tract. These suppressor mutations affected primarily the second step of splicing in vitro. These results support a specific role for the polypyrimidine tract in the second step of splicing and confirm that, in a biological system, uridines and cytosines are not functionally equivalent within the polypyrimidine tract. Unlike the wild-type virus, the second-step mutants displayed significant levels of lariat-exon 2 in vivo, suggesting a role for splicing intermediates in regulation. Our results indicate that splicing regulation can involve either the first or second step.

Pre-mRNA splicing involves the accurate removal of introns and joining of exons (see references 14, 28, and 37 for reviews). In higher eukaryotes, these reactions require several degenerate *cis*-acting signals: the 5′ splice site (AG/GURAGU), the 3′ splice site (CAG/G), the branch point sequence (BPS; YNYU RAC), and the polypyrimidine tract $(Y)_n$ (Fig. 1A). These signal sequences are recognized by nuclear *trans*-acting factors: small nuclear ribonucleoprotein particles (snRNPs) and non-snRNP protein factors. The U1, U2, U4, U5, and U6 snRNPs and other factors bind directly, or indirectly, to the pre-mRNA in an ordered manner, ultimately forming a large complex known as the spliceosome. The U1 snRNP initially recognizes the 5′ splice site, and the U2 snRNP recognizes the BPS, both through RNA-RNA base pairing. The polypyrimidine tract is required for spliceosome formation, and one function of this element is to recruit a protein, U2AF, that stabilizes the binding of the U2 snRNP (21, 49). The polypyrimidine tract may also play an indirect role in selecting the 3′ splice site through a scanning mechanism (40, 42). The functional strength of the polypyrimidine tract has been correlated with its length, pyrimidine content, and context (8, 10, 29, 36, 38).

In vitro splicing studies have revealed that the splicing reaction proceeds through two chemical steps (Fig. 1A). In the first step, the phosphate at the 5′ splice junction is attacked by the 2′ OH of an adenosine residue (the branch point), usually located between 18 and 40 nucleotides upstream of the 3′ splice site. This reaction produces two intermediates, exon 1 and lariat-exon 2. The efficiency of the first step can be influenced by the extent of base pairing between the BPS and the U2 small nuclear RNA (snRNA) (47, 50, 51). The most efficient BPS (UACUAAC; the branch point is underlined) is one that will pair perfectly with the U2 snRNA (50). Pairing may induce bulging of the branch site A residue, and this topology may play a role in its selection (35). In the second step, the newly created 3′ OH group at the end of exon 1 attacks the phosphate at the 3′ splice junction, thereby joining the two exons and releasing the lariat intron. Recent studies using yeast and mammalian systems have revealed the existence of a dynamic network of RNA base-pairing and RNA-protein interactions within the spliceosome that serve to juxtapose the 5′ and 3′ splice sites and perhaps catalyze both of the chemical steps in splicing (see references 28, 30, and 43 for recent reviews).

In constitutive splicing, in accordance with the pathways described above, splice sites are chosen in a pairwise manner, such that neighboring exons are joined. Alternative splicing is a regulatory mechanism that involves conditional splicing of certain introns in order to produce different mRNAs from a single pre-mRNA species (for reviews, see references 14, 15, 23 to 25, and 41). The inclusion or exclusion of exons is controlled in a tissue-specific or developmentally regulated manner. Alternative splicing requires that the normal pairwise selection of neighboring exons be overridden, as exemplified by exon skipping or intron retention. The mechanisms can involve a competition between strong and weak splice sites that establishes a default splicing pattern (for reviews, see references 23 and 24). Specific, or generic, factors can then override the default pattern to produce the tissue-specific pattern.

* Corresponding author. Mailing address: Fox Chase Cancer Center, Institute for Cancer Research, 7701 Burholme Ave., Philadelphia, PA 19111. Phone: (215) 728-3668. Fax: (215) 728-2778.

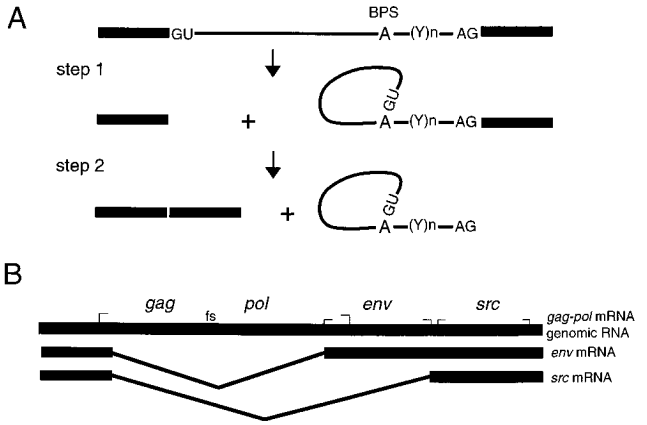

FIG. 1. (A) Diagram of the two steps in the splicing reaction. (See the text for details.) The conserved GU and AG at the intron borders are shown. The branch point A residue is shown, and (Y)n denotes the polypyrimidine tract. (B) RNA splicing pattern for ASV. Incomplete splicing, as well as alternative splicing, is required to coexpress the RNA species shown. (See the text for details.) Gene borders are indicated by brackets. *gag* encodes the structural proteins and protease, *pol* encodes reverse transcriptase and integrase, and *env* encodes the viral envelope proteins. *gag* and *pol* are translated from the full-length RNA, the latter by occasional translational frame shifting (fs), while *env* is translated from a spliced RNA. The nonessential *src* oncogene product is translated from a separate mRNA, and regulation of this splicing event has been addressed by others (44).

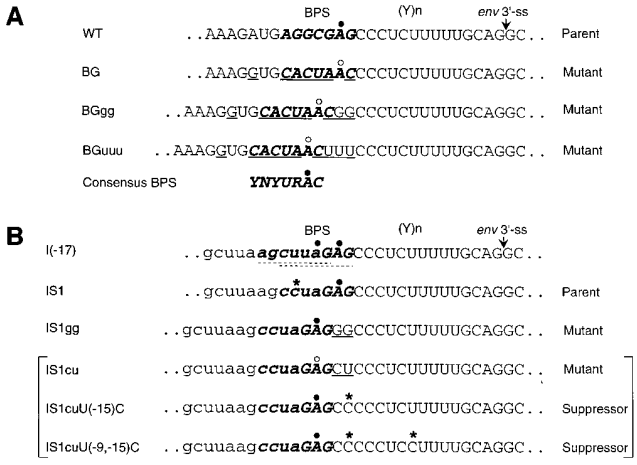

FIG. 2. Sequence of the ASV *env* 3′ splice site (ss) regions addressed in this paper. The BPS is indicated in boldface italic type. The multiple BPSs used in I(−17) are indicated by dashed underlining. The polypyrimidine tract is in the region designated (Y)n. Oligonucleotide-directed mutations introduced in this study are underlined. (A) Mutations based on wild-type ASV. The branch point A residue that has been mapped in vitro (9) is indicated by the filled circles. Open circles indicate predicted branch points for various mutants. An A-to-G mutation outside the BPS was included in order to introduce a diagnostic restriction site. (B) Mutations based on the IS1 parent. Lowercase letters in the sequence indicate the inserted nucleotides in the I(−17) oversplicing mutant. IS1 differs from the I(−17) sequence by the U-to-C suppressor mutation at position −20 from the splice site (asterisk). Asterisks also indicate polypyrimidine tract suppressor mutations isolated after transfection with the IS1cu oversplicing mutant. Filled circles indicate branch points mapped in vivo (see Results). I(−17) and IS1 branch points have been previously mapped in vitro (9). An open circle indicates the predicted branch point in IS1cu. Brackets indicate that suppressor mutations were derived from the IS1cu mutant.

Retroviruses employ a novel form of regulated splicing that provides an economical strategy for gene expression (7). They produce a single primary transcript that minimally encodes the three essential replicative genes, 5′-*gag-pol-env*-3′. In the avian sarcoma virus (ASV), approximately one-third of the molecules are spliced to remove the *gag-pol* region (Fig. 1B). This brings the *env* coding region to the 5′ position to allow translation of the viral surface proteins (*env* gene products). The remaining full-length molecules escape splicing and are transported to the cytoplasm, where they are translated to produce the retroviral core proteins and enzymes. Some unspliced RNA is also assembled into progeny virions to serve as the genetic material. The existence of these alternative pathways implies that some primary retroviral transcripts either never enter the splicing pathway or are released before commitment to splicing occurs. In simple retroviruses, it appears that the balance between spliced and unspliced forms is maintained by weak splice sites (9, 17, 19, 26) as well as other *cis*-acting elements (1, 27, 44).

We previously showed that in the ASV system, a suboptimal BPS is essential to maintain a balance between *env* mRNA and unspliced RNA (9, 17, 19). In vitro splicing experiments demonstrate that a weak branch point at position −16 from the *env* splice acceptor site was used (BPS, AGGCGAG; positions −21 through −15; the branch point is underlined) (Fig. 2A). Only trace amounts of lariat-exon 2 could be detected in vitro, indicating a major block prior to the first step of splicing. A 24-bp insertion mutation which interrupts the BPS was introduced at position −17 from the *env* splice acceptor site [designated I(−17)]. This mutation is useful in terms of the complete viral life cycle because, in contrast to the wild-type virus, the region between −22 and −1 of the *env* 3′ splice site is noncoding and therefore can accept additional mutations without interfering with the viral *pol* gene. However, this insertion activated the −16 branch site and provided a second branch site at −18 within the inserted sequence. This resulted in overproduction of *env* mRNA at the expense of the full-length RNA and a concomitant virus replication defect. The spontaneous mutation rate of retroviruses is relatively high; immune-escape and drug-resistant mutants can be readily isolated in tissue culture systems (see reference 18 for a review). Accordingly, we were able to isolate spontaneous suppressor mutations that restored both viral growth and balanced splicing, and these mapped to either the new BPSs or positive elements in the neighboring exon (9, 17, 19; also see references 45 and 48). Since incomplete splicing must be maintained for virus viability, the selection is for weakened, but functional, *cis*-acting splicing signals.

In this report, we extend our analysis of a novel BPS suppressor mutation [insertion suppressor 1 (IS1) (Fig. 2B) (17, 19); also designated T/C(−20) in reference 9]. The branch point was mapped in vitro and corresponded to the A residue at −16, as in the wild type, but was situated in an altered BPS context (**CCUA**G**A**G; the net BPS sequence changes from the wild type are in boldface type). Interestingly, in vitro analysis showed that this new BPS was used efficiently in the first step of splicing but the lariat-exon 2 intermediate containing this branch site appeared to be a poor substrate for ligation to exon 1. In this study, we have exploited this mutant to investigate the second step of splicing. We show that the second-step block can be overcome by extending the polypyrimidine tract. The block was restored by a genetically selected suppressor mutation consisting of a single U-to-C transition in the pyrimidine tract. All of the second-step mutations characterized in vitro produced high levels of lariat-exon 2 in vivo. These and other results suggest a role for intermediates in splicing regulation.

MATERIALS AND METHODS

Plasmids. For in vivo experiments, an infectious DNA clone of the Schmidt-Ruppin B strain of ASV, pLD6, was used (17). For preparation of in vitro splicing substrates, an ASV *env* minigene was constructed by using the pSP73 vector. The strategy was similar to that described previously (9). The region from nucleotide 268 to 547 (encompassing the 5′ splice site at position 397/398) was amplified from ASV clone pATV8-K by PCR. (The sequence is numbered as described by Schwartz and Gilbert [39].) The PCR primers were designed to introduce a *Sal*I restriction site at the left end and an *Asp*718I site at the right end. The fragment was inserted in the polylinker region of pSP73 at the corresponding sites. The resulting intermediate plasmid was cleaved with *Asp*718I and *Eco*RI, and a ca. 2-kbp *Asp*718I-*Eco*RI fragment from pLD6 was inserted. This fragment included 77 bp of the intron, the *env* 3′ splice, and a large portion of the *env* gene. Two other mutations that eliminated two *Ban*II sites within the vector portion of the plasmid were introduced. This left a unique *Ban*II site remaining at the junction of the BPS and polypyrimidine tract (..GAGCCC..). In site-specific mutagenesis experiments, plasmids that had lost this restriction site could be selected. The final construct, pSP73ASV, contained a first exon of ca. 130 bp, an intron of 226 bp, and a large *env* exon. A second version of pSP73ASV that contained the IS1 suppressor mutation described previously was constructed (17).

Mutagenesis. Site-directed oligonucleotide mutagenesis was carried out as described previously (16). All mutations were confirmed by nucleotide sequence analysis using the Sequenase method (2). The mutations are illustrated in Fig. 2.

Transfection and RNA analysis. Cell propagation and transfections were carried out as previously described (17). For virus replication experiments, chicken embryo fibroblasts were transfected by the DEAE-dextran method and were passaged when necessary. For transient transfection experiments, the QCl-3 quail cell line was used (17). RNA was prepared by the guanidium method (2) and was analyzed by S1 analysis as described previously (17, 19). The homologous DNA probe was used for each mutant RNA. Bands were quantified with a Fuji BAS 1000 Bio-Imaging Analyzer.

In vitro splicing substrates and reactions. The reactions were carried out as described previously (9). The pSP73ASV vector or its derivatives were linearized with *Hpa*I to produce a runoff transcript of ca. 500 nucleotides. Splicing reactions produced a free exon 1 (ca. 130 nucleotides), a lariat-exon 2 intermediate which migrated more slowly than the precursors, and a spliced product of ca. 279 nucleotides. The β-globin transcript has been described previously (9).

PCR, cloning, and sequencing. For cloning and sequence analysis of potential suppressor mutations, virus particles were collected and DNA was synthesized by using an endogenous reverse transcriptase reaction. Virus particles were collected from media (5 ml) by centrifugation and were added to a standard reverse transcription reaction mixture containing 100 mM Tris-HCl (pH 8.0), 25 mM NaCl, 3 mM magnesium acetate, 30 mM dithiothreitol, 0.05% Nonidet P-40, and 1 mM deoxynucleotide triphosphates. EGTA [ethylene glycol-bis(β-aminoethyl ether)-*N*-*N*-*N*′-*N*′-tetraacetic acid] was included at a concentration of 1 mM by the method of Borroto-Esoda and Boone (3). Viral DNA was purified by proteinase K treatment, phenol extraction, and ethanol precipitation in the presence of a tRNA carrier. The PCR primers chosen overlapped with existing restriction sites flanking the *env* splice acceptor site at nucleotide positions 5077/5078: *Asp*718I (position 5000 on the upstream side) and *Hpa*I (position 5186 on the downstream side). The regions were amplified (25 cycles), cleaved with *Asp*718I and *Hpa*I, and cloned in the pSP73ASV vector. Individual clones were picked, and the amplified region was sequenced with the Sequenase system (United States Biochemical). For genetic tests, segments containing putative suppressor mutations were transferred from pSP73ASV to the pLD6 clone by using a 2-kb *Asp*718I-*Cla*I fragment.

Primer extension. The primer extension reactions were carried out essentially as described previously (2). End-labelled primer (10^6 dpm, 5 pmol) and 16 μg of total cellular RNA were mixed in hybridization buffer. The mixture was incubated at 45°C for 2 h for primer annealing. The extension reaction was carried out, with avian myeloblastosis virus reverse transcriptase (Life Sciences) used as described previously (2) at 43°C for 90 min. The products were analyzed on a 6% polyacrylamide sequencing gel containing 7 M urea.

RESULTS

The wild-type ASV *env* polypyrimidine tract can support efficient splicing in the presence of a strong BPS. The wild-type ASV *env* branch point is weak, and only trace amounts of splicing intermediates and products can be detected in vitro (9). This observation parallels the incomplete splicing observed in vivo and indicates that regulation occurs prior to the first step of splicing. In addition to a poor match of the wild-type BPS with the U2 snRNA, the major branch point A residue is unusually close to the 3′ splice site (position −16, in contrast to the consensus distance of between −18 and −38) (Fig. 2A). The extent to which this feature might contribute to splicing regulation was unknown. In contrast to the wild type, the IS1 mutant displayed efficient branch formation at position −16 in vitro, which is consistent with the improved match to U2 snRNA (9). However, the resulting lariat-exon 2 intermediate was not efficiently used for exon ligation. Since IS1 contains the wild-type polypyrimidine tract, these results indicated that the polypyrimidine tract was capable of providing those functions required for efficient branch formation. To further test this idea, we replaced the wild-type ASV *env* BPS with the mouse β-globin intron 1 BPS (AGGCGAG changed to CAC UAAC). These changes are predicted to provide five base pairs with U2 snRNA, versus the two base pairs predicted for wild-type BPS. The predicted branch point A residue remained at position −16 (BG sequence in Fig. 2). Wild-type and mutant substrates were transcribed in vitro and incubated in a HeLa cell splicing extract, as described earlier (9) (Fig. 3A). As noted previously (9), less than 5% of the wild-type substrate is spliced in vitro, and some degradation is noted during the incubation period (Fig. 3A, lanes 3 and 4). In contrast, approximately 30 to 50% of the analogous substrate containing the β-globin BPS, ASV-BG, is spliced (lanes 5 and 6). We conclude that the wild-type polypyrimidine tract is efficient in conjunction with a strong BPS. Extending the polypyrimidine with a UUU insert (BGuuu sequence in Fig. 2) did not appear to further activate splicing in vitro (Fig. 3A, lanes 7 and 8).

The ASV-BG mutations were transferred to a cloned viral DNA genome, and the in vivo splicing patterns were examined after transient transfection of avian cells by means of an S1 nuclease protection assay (Fig. 3B). The results show that the ASV-BG mutation caused a significant up-regulation of splicing compared with that of the wild type (compare lanes 2 and 3). The ASV-BGgg mutation (Fig. 2), which altered the splice

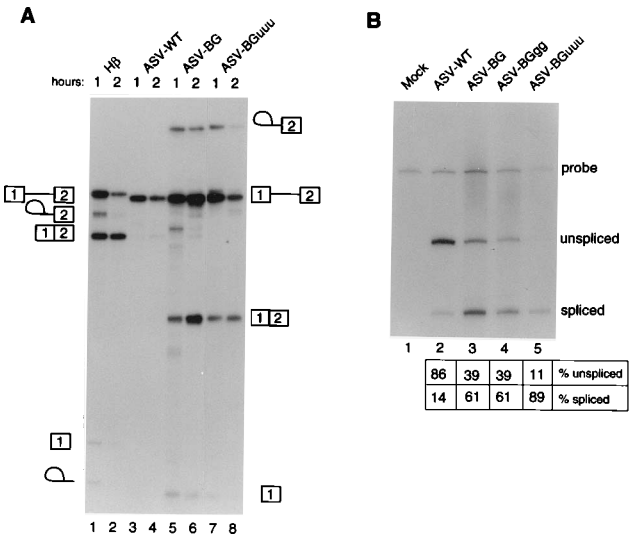

FIG. 3. (A) In vitro splicing of ^{32}P-labelled RNA substrates prepared from the pSP73ASV vector and derivatives. The splice site mutations contained within each substrate (Fig. 2) are indicated above the lanes. Lanes 1 and 2, human β-globin (Hβ) substrate used as a control. Lanes 3 to 8, pSP73ASV wild type (WT) and derivatives. The positions of splicing intermediates and products are shown on the left for Hβ and on the right for ASV derivatives. Exons are indicated by numbered boxes, and the lariat structure is shown as a loop. (B) In vivo splicing of ASV-WT and BPS mutants as measured by an S1 nuclease assay for *env* mRNA (see Materials and Methods). QCl-3 cells were transfected with the indicated clones, and RNA was harvested at 60 h posttransfection. The quantitation data are shown below the lanes. The differences in total intensity between lanes reflect differences in transfection efficiencies and the fact that different S1 probes had to be used for each virus. Mock, mock transfection.

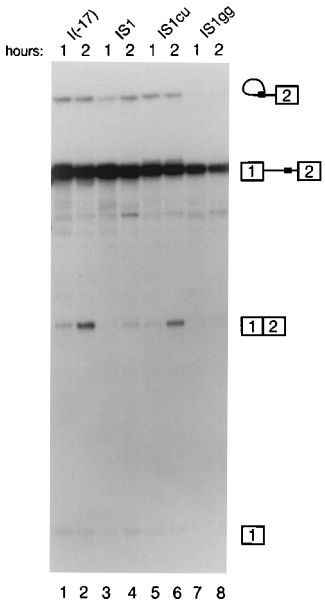

FIG. 4. In vitro splicing of IS1 and derivatives. Mutations are indicated above lanes. Procedures and symbols are as described for Fig. 3A. A filled box in the splicing substrate indicates the original insertion mutation in I(−17).

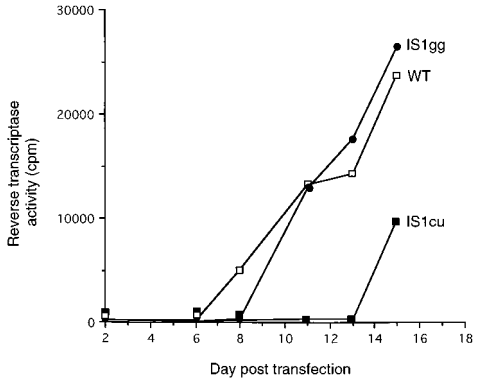

FIG. 5. Replication of *env* splice site mutants. Chicken embryo fibroblast cells were transfected on day 0 with the ASV DNA clone pLD6 (ASV-WT) or derivatives of ASV-IS1 (as indicated). The supernatants were collected on the indicated days and assayed for virion-associated reverse transcriptase activity (17).

site-branch point spacing as well as the composition of the polypyrimidine tract, had no effect on splicing, in contrast with the BG mutation alone. However, the BGuuu mutation caused a further up-regulation of splicing in vivo (Fig. 3B, lane 5). These results confirm that wild-type *env* splicing regulation involves a suboptimal BPS and that the wild-type polypyrimidine tract is efficient in the context of a strong BPS. However, lengthening of the polypyrimidine tract (BGuuu) appears to further activate splicing in vivo.

Since the BG mutations were made in the wild-type background, the *pol* coding region was altered. The corresponding viral DNA constructs, used in the transient expression experiments illustrated in Fig. 3B, were unable to produce infectious virus after transfection of susceptible cells. We cannot discern whether the replication defect is due to a splicing imbalance, a disruption of *pol* function, or both. Studies using the IS1 parent virus circumvent this problem, since the *env* 3′ splice site region is noncoding.

Effects of polypyrimidine tract mutations on the second step of splicing. As described above, the IS1 suppressor mutation acts primarily at the second step of splicing in vitro. Figure 4 shows the in vitro splicing activity of the I(−17) oversplicing parent compared with that of the IS1 suppressor (compare lanes 1 and 2 with 3 and 4). The IS1 suppressor differs by a single nucleotide change from the I(−17) parent (U to C at −20 from the splice acceptor [Fig. 2B]). Although the wild-type pyrimidine tract can support efficient splicing in the presence of a strong BPS (as noted above), we asked whether the polypyrimidine tract could play a specific role in the second-step block of mutant IS1. The polypyrimidine tract was extended by insertion of two pyrimidine residues, CU, between the BPS and the existing polypyrimidine tract (denoted IS1cu in Fig. 2). This insertion also repositions the expected branch point from −16 to −18. In vitro, the IS1cu mutant (Fig. 4, lanes 5 and 6) exhibited greater exon ligation activity than the IS1 parent (lanes 3 and 4). These results suggest a specific role for the polypyrimidine tract in the second step of splicing. In contrast to the CU insertion, a GG insertion at the same position in IS1 (IS1gg sequence in Fig. 2) resulted in a reduction in the levels of both lariat-exon 2 and ligated exon (Fig. 4, lanes 7 and 8). Thus, the CU mutation relieved the second-step block while the GG insertion appeared to inhibit the first step. On a longer exposure than that of the film in Fig. 4, we could detect lariat-exon 2, but not the spliced product, in lane 8. This result suggests that the second-step block is maintained in IS1gg.

Lengthening of the polypyrimidine tract results in splicing activation in vivo and a replication defect. The IS1cu and IS1gg mutations were transferred to the infectious viral DNA clone, pLD6. Susceptible chicken embryo fibroblasts were transfected, and the cultures were monitored for virus production by a reverse transcriptase assay (Fig. 5). Under the conditions used, virus cannot be detected unless multiple rounds of infection occur. (The IS1 suppressor virus replicates at a rate similar to that of the wild type; in this experiment, the wild type was used as a control.) Wild-type virus was detected by day 9 posttransfection. In contrast, virus was detected in only one of six transfections with the IS1cu construct and, in this case, there was a significant delay in the appearance of the virus (Fig. 5; discussed further below). The IS1gg mutation had no significant effect on replication. To determine whether the replication defect in IS1cu reflected a splicing defect, RNA was examined in a transient transfection assay that was not dependent on viral replication (Fig. 6A). The IS1cu mutant showed a dramatic increase in the efficiency of *env* splicing (lane 4) over that of the IS1 parent. Thus, extension of the polypyrimidine tract by 2 nucleotides activated splicing, both in vivo and in vitro, and also produced a replication defect. In contrast, the IS1gg mutant was replication competent and the results in Fig. 6B show that this mutation resulted in reduced splicing efficiency in vivo, compared with the IS1 parent or wild type (compare lanes 2 and 3 of panels A and B). Apparently, this down-regulation of *env* splicing does not affect replication efficiency (Fig. 5).

Selection for inefficient splicing results in suppressor mutations in the polypyrimidine tract. If the defect in the IS1cu mutant was due to oversplicing, we considered that spontaneous suppressor mutations might arise (17). The delayed appearance of replication-competent virus in the IS1cu-transfected cultures was consistent with this possibility (Fig. 5). Virus particles were collected during the experiment illustrated in Fig. 5, and cDNA was synthesized by using the endogenous reverse transcriptase reaction (see Materials and Methods).

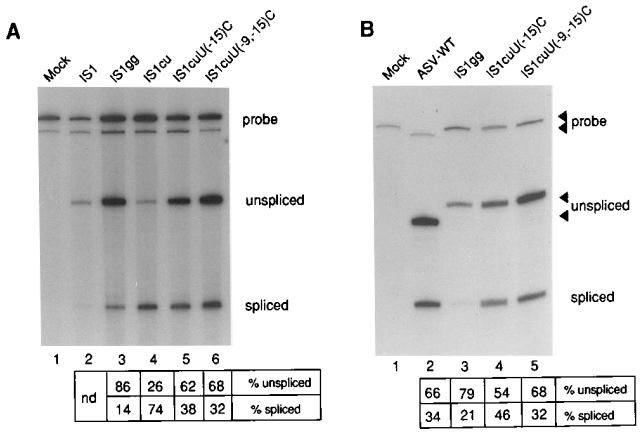

FIG. 6. In vivo splicing of IS1 derivatives. Unspliced and spliced *env* mRNAs were detected as described for Fig. 3B. (A) Transient transfection of viral constructs. Since the IS1cu parent is replication defective and genetically unstable, a transient transfection assay was used to compare IS1cu with the indicated constructs. The quantitation data are shown below the lanes. The signal for IS1 was weak in this experiment, and thus an accurate ratio could not be determined (nd). (The intensity of the total signal varies between lanes as explained for Fig. 3B.) Mock, untransfected cells. (B) Analysis of viral RNA from infected chicken embryo fibroblast cells. Infection was initiated by transfection with the indicated viral DNA clones. Infectious virus produced from the initial transfection then spread within the culture. Cells were passaged until they appeared transformed (ca. 1 week). RNA for the Mock lanes was prepared from uninfected cells. The relative amounts of unspliced and spliced RNAs are quantitated below the lanes. Differences between lanes in the total intensity reflect the use of different S1 probes and the percentage of cells in the culture that were infected at the time of harvest. Arrowheads indicate expected size differences due to the IS1 insertion mutation.

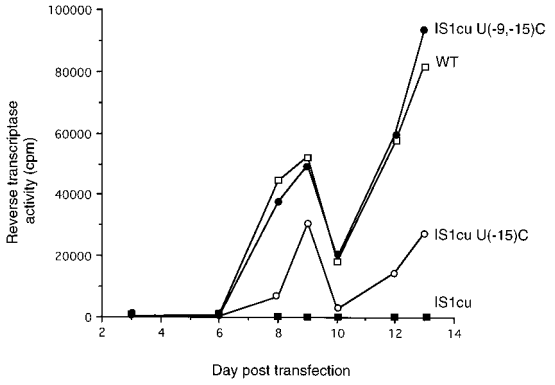

FIG. 7. Replication of *env* splice site mutants. Reverse transcriptase activity was measured as described in the legend for Fig. 5. Mutations are indicated. The drop in activity at day 10 was due to dilution of cells during passage. WT, wild type.

This DNA then served as a template to amplify the 180-bp *env* 3′ splice site region by PCR, and the resulting products were molecularly cloned. Sequence analysis showed that six of seven clones contained a single base change from the IS1cu parent within the *env* 3′ splice site region: the inserted U at position −15 was changed to a C [denoted by U(−15)C in Fig. 2]. The remaining clone contained two changes: the same U(−15)C change plus a second U-to-C change at position −9 within the polypyrimidine tract [denoted by U(−9,−15)C in Fig. 2]. The presence of the U(−15)C change could be inferred by the loss of a *Sac*I restriction site that was introduced with the CU insertion in IS1cu. The population of PCR-generated fragments was resistant to *Sac*I (data not shown), which is consistent with the presence of the U(−15)C mutation in the majority of mutant viral genomes.

To determine if the changes in the polypyrimidine tract were the sole mutations responsible for the revertant phenotype, the segments encompassing the *env* splice acceptor region were transferred back to a wild-type viral DNA clone. The resulting viral clones contained either the U(−15)C single suppressor mutation or the U(−9,−15)C double mutation in the IS1cu background. These two constructs, along with the IS1cu parent, were used to transfect susceptible chicken cells (Fig. 7). In this experiment, no replication-competent virus was detected after transfection of the IS1cu parent. In contrast, transfection of the IS1cuU(−9,−15)C double suppressor resulted in rapid appearance of infectious viruses, indicating that these two changes were sufficient to suppress the IS1cu mutation. Transfection with the clone carrying only the U(−15)C mutation displayed an intermediate growth phenotype (partial suppression). PCR amplification, followed by sequence analysis, confirmed that these suppressor mutations were stable during the course of this experiment (data not shown). These results demonstrate that the pyrimidine tract transitions are solely responsible for the revertant phenotype.

Effects of polypyrimidine tract suppressor mutations on splicing efficiency. The effects of the suppressor mutations on splicing were measured in vivo by transient transfection, as for Fig. 3B (Fig. 6A, compare lanes 4, 5, and 6). The single suppressor mutation, U(−15)C, reversed the oversplicing phenotype of the IS1cu parent (ca. 38% spliced versus ca. 74% spliced, respectively). In both transiently transfected cells (Fig. 6A), and chronically infected cells (Fig. 6B), the presence of the second U-to-C transition at −9 had a modest but detectable effect. Thus, the U(−15)C suppressor is sufficient for replication and the second mutation may provide some additional selective advantage. We conclude that U and C residues in the polypyrimidine tract are not functionally equivalent.

The effects of the suppressor mutations were also assayed in vitro as described above (Fig. 8). Both the single- and double-suppressor mutations significantly reduced splicing compared with the IS1cu parent (compare lanes 4, 6, and 8). As is the case for the original parent, IS1, the block appears to occur mainly in the second step of splicing. Again, these results

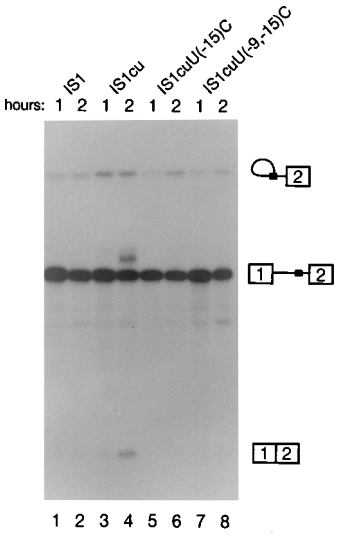

FIG. 8. In vitro splicing analysis of IS1cu suppressor mutations. Details of the procedures and symbols are as described for Fig. 3 and 4.

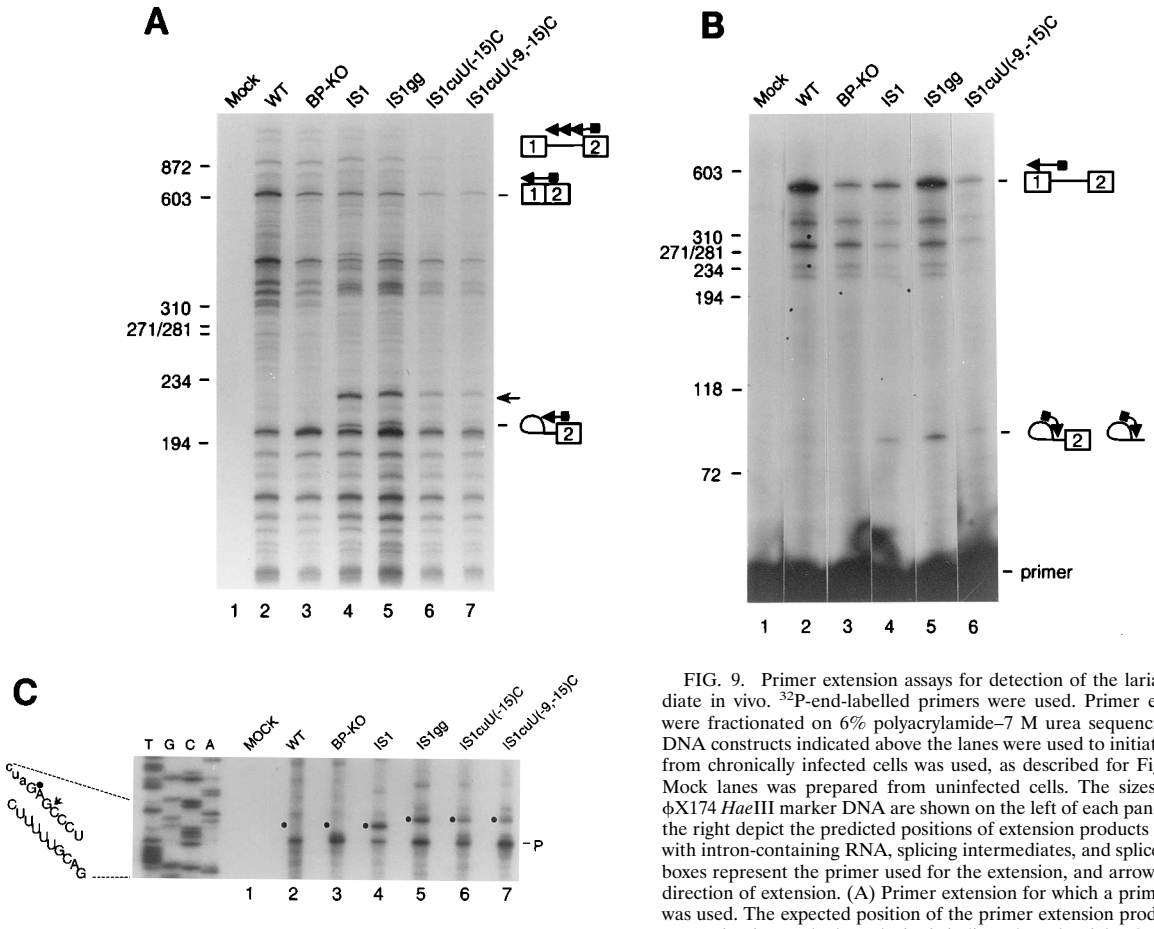

FIG. 9. Primer extension assays for detection of the lariat-exon 2 intermediate in vivo. ^{32}P-end-labelled primers were used. Primer extension products were fractionated on 6% polyacrylamide–7 M urea sequencing gels. The viral DNA constructs indicated above the lanes were used to initiate infections. RNA from chronically infected cells was used, as described for Fig. 6. RNA for the Mock lanes was prepared from uninfected cells. The sizes and positions of ϕX174 *Hae*III marker DNA are shown on the left of each panel. The symbols on the right depict the predicted positions of extension products that are consistent with intron-containing RNA, splicing intermediates, and spliced products. Filled boxes represent the primer used for the extension, and arrowheads indicate the direction of extension. (A) Primer extension for which a primer site in the exon was used. The expected position of the primer extension product corresponding to termination at the branch site is indicated on the right. On this short gel, the bulk of this product migrated aberrantly (arrow) (see panel C). (B) Primer extension for which a priming site in the intron was used. This primer detects both free lariat and lariat-exon 2 (see symbols on the right), as well as a debranched intron. (C) Fine mapping of primer extension products shown in panel A. Products from panel A were coelectrophoresed with a sequence ladder (lanes T, G, C, and A) derived from IS1. Sequencing was carried out by the dideoxy method, using the same ^{32}P-labelled primer that was used for the extension assays. The sequence of the branch point region is shown on the left. Lowercase letters indicate the insertion mutation in IS1, as in Fig. 2; the expected major branch point A residue for IS1 (and the wild type) is indicated by a filled circle, also as in Fig. 2. The positions of expected branch points are indicated next to each lane by the filled circle. The extension product seen with IS1, which is absent in the wild type (WT), corresponds to the major branch point mapped in vitro (9). (In panel A, the bulk of this product apparently migrated anomalously, presumably because of incomplete denaturation.) The second-step mutants in lanes 5 to 7 show extension products that are 2 nucleotides longer than with IS1, corresponding to a stop at the same branch point. This result is expected because of the GG and CU inserts (the insertion site is indicated by the arrow in the sequence on the left). A likely reverse transcriptase pause site (P) in the primer extension that is common to all samples is indicated.

support a role for the polypyrimidine tract in the second step, since lariat-exon 2 and exon 1 intermediates are present but the amount of spliced product is greatly reduced. It should be noted that the levels of intermediates observed for IS1, IS1cuU(−15)C, and IS1cuU(−9,−15)C do not accumulate beyond those observed for IS1cu. [A similar relationship between IS1 and I(−17) can be noted in Fig. 4.] Thus, although the suppressor mutations clearly affect the second step, there may be additional consequences of this block. For example, these suppressor mutations may also have some effect on the first step; this would not be surprising, since the polypyrimidine tract is required for this step.

Suppressor mutations affect the second step of splicing in vivo. In vitro splicing reactions (Fig. 8) indicated that the IS1 parent and the IS1cu suppressors were blocked primarily in the second step. In contrast, wild-type *env* splicing appears to be regulated at the first step (Fig. 3A, lanes 3 and 4) (9). To assess the biological relevance of the second-step blocks observed in vitro, we assayed for accumulation of lariat-exon 2 in virus-infected cells using a standard reverse transcription-primer extension assay (Fig. 9). The extension reaction cannot proceed through the branched nucleotide in the template strand, and thus the length of the extension product can be used to map the branch site. One primer was positioned in the *env* exon such that extension products that terminated at the expected IS1 branch site (position −16) should be 205 nucleotides long. The extension reactions produced a number of bands; most are presumably due to strong secondary structure of the RNA template, especially in the region between the primer site and the splice acceptor site. A discrete product which corresponded to the expected runoff for the spliced *env* transcript (604 nucleotides) was detected (Fig. 9A, lanes 2 to 7). A major extension product (Fig. 9A, arrow) was detected with RNA from IS1-infected cells (lane 4) but was not detected in wild type-infected cells (lane 2). This product was also absent from another replication-competent virus containing a branch point mutation (BP-KO [3a]) (lane 3). However, the product was seen with other mutations that are associated with a second-step block in vitro (lanes 5 to 7). In Fig. 9A, the novel extension products migrated more slowly than expected for the 205-nucleotide product that would be diagnostic for the lariat-exon

2 intermediate (see the Fig. 9 legend). However, on a longer sequencing gel (Fig. 9C), an adjacent sequence ladder showed that the novel extension product in IS1 corresponded to the −16 branch point detected in vitro (Fig. 9C, lane 4; Fig. 2; also see reference 9). The same branch site is predicted for the wild type, but no extension product is visible (Fig. 9C, lane 2). For IS1cuU(−15)C, IS1cuU(−9,−15)C, and IS1gg, this product is detected and is shifted by 2 nucleotides, which is consistent with the CU and GG dinucleotide insertions.

To confirm the accumulation of lariat-exon 2 intermediates in vivo, we used a second primer, positioned in the intron (Fig. 9B). In this case, an extension product of 97 nucleotides would be consistent with the lariat-exon 2 intermediate; however, this product is not diagnostic since it could also indicate the presence of a free lariat (or a stable debranched intron). For all viruses, we detected a major extension product consistent with the 494-nucleotide runoff expected for unspliced RNA. We also detected an extension product of ca. 100 nucleotides with RNA from cells infected with the predicted second-step mutants (Fig. 9B, lanes 4 to 6). Electrophoresis with an adjacent sequence ladder confirmed that the shorter extension products corresponded to the 5′ end of the intron (data not shown). This 97-nucleotide product was not readily detected with RNA from wild type-infected cells or from cells infected with the aforementioned BP-KO mutant (lanes 2 and 3). We estimate from the data in Fig. 9B that lariat-exon 2 may represent as much as one-fifth of the level of full-length RNA. Results obtained with both primers demonstrate that viral lariat-exon 2 intermediates are detected only in cells infected with the predicted second-step mutants and that they are present at high levels relative to those of unspliced RNA.

DISCUSSION

Simple retroviruses provide a useful model for studying pre-mRNA splicing. They produce a single RNA transcript that can be either spliced or transported to the cytoplasm with all its introns intact. This is in contrast to cellular pre-mRNAs, whose splicing and transport are usually tightly coupled. It is of interest to understand how some retroviral RNA molecules escape splicing. In simple retroviruses, this regulation does not appear to require viral proteins (1, 19, 27) and may involve a release of molecules from the splicing pathway. It has been shown in some model systems that mutation of both splice sites is sufficient to release RNA from the nucleus (see reference 5 for a review). Our previous work showed that ASV *env* splicing regulation involved a weak BPS (9). These results support a model for regulation of wild-type ASV splicing in which some full-length RNA is released from the splicing pathway because of weak interactions with the splicing machinery. Many regulated introns are now known to contain weak splice sites. Here, we show that converting the suboptimal ASV BPS to a β-globin BPS activates splicing, both in vitro and in vivo, and this is consistent with our general model. Although weak splice sites and other *cis*-acting signals (1, 27, 44) may cause the release of retroviral transcripts from the splicing pathway, transport of unspliced ASV RNA to the cytoplasm may require additional *cis*-acting signals (4). For human immunodeficiency virus type 1, a complex retrovirus, expression of unspliced RNA and *env* mRNA requires a *trans*-acting viral protein, Rev, and the cognate *cis*-acting target sequence, the Rev-responsive element (RRE). Although the mechanism is not fully understood, there is evidence that the Rev protein promotes release of RRE-containing RNAs from the splicing pathway (20, 22).

We have observed previously, as well as in this work, that oversplicing of ASV *env* mRNA results in a viral replication defect. We believe that the replication defect is caused by depletion of the full-length RNA which serves as both *gag-pol* mRNA and genomic RNA. We have been able to isolate suppressor mutations that down-regulate splicing and thus restore levels of unspliced RNA. We originally isolated two general classes of suppressors (9, 17, 19): class 1 affected the BPS region, while class 2 mutations were deletions of positive splicing elements present within the 3′ exon (45, 48). The pseudorevertant viruses carrying these suppressor mutations regulate splicing by mechanisms distinct from those of the wild-type virus (9). Although these suppressor mutations were selected by virus passage in avian cells, we found that their relative effects on splicing could be recapitulated in vitro by using HeLa cell-derived splicing extracts. These results indicate that the suppressor mutations affect general interactions with the splicing machinery. Also, genetic selection has revealed simple, but potent, sequence changes that are amenable to further biochemical studies. For example, the polypyrimidine tract appears to bind several protein factors and the mutations described here may alter the affinity for one or more of these factors (as discussed below).

The IS1 suppressor mutation was of particular interest because regulation appeared to be at the second step of splicing and thus could serve as a biologically relevant model to study interactions that are unique to this step. We are aware of only one other system where a block in the second step may be relevant to splicing regulation. This is the T-cell receptor β gene, for which partially spliced transcripts containing lariats accumulate in the nucleus (34).

The mechanism of the second-step block in IS1 is unknown. For example, we considered that the IS1 polypyrimidine tract (which is identical to that of the wild type) was not fully competent for the second step of splicing. However, in conjunction with a strong β-globin BPS (the ASV-BG mutation), this polypyrimidine tract appears to be efficient. Since the BPS-polypyrimidine tract can be viewed as a functional unit (36, 40), it seems that the relative strength of each constituent, and its context, may contribute to the net splicing phenotype of IS1. The second-step block in IS1 could be overcome, in vitro, by extending the polypyrimidine tract with a CU insertion. This mutation also up-regulates splicing in vivo. These observations suggest that the polypyrimidine tract plays a specific role in the second step of splicing, as also proposed by Reed (36). In contrast to the CU insertion, an analogous GG insertion reduced splicing efficiency. These results are also in agreement with published work which showed that splicing was most efficient when the BPS was immediately adjacent to the polypyrimidine tract (36). Both the CU and the GG insertions repositioned the predicted branch site from −16 to −18 from the 3′ splice site, the latter position being a better fit to the consensus distance. It is difficult to discriminate between spatial and sequence effects of these inserts; we cannot rule out the possibility that the CU insertion relieves a steric constraint between the BPS and the 3′ splice site.

Analysis of suppressor mutations of IS1cu confirmed a specific role for the polypyrimidine tract in the second step of splicing. The U(−15)C suppressor affects the inserted uridine, and this mutation is sufficient to down-regulate splicing in vivo. The U(−9,−15)C double suppressor shows a small but measurable decrease in splicing efficiency in vivo compared with that of the U(−15)C single suppressor. In vitro, the U(−15)C and U(−9,−15)C suppressor mutations mainly affect the second step of splicing. These results also indicate that U and C residues are not functionally equivalent within the polypyrimidine tract. A similar conclusion was also drawn by Roscigno et al. (38), who carried out a systematic mutagenesis of the poly-

pyrimidine tract. However, in their model system, multiple changes were required to observe significant effects and these effects were manifested at the first step. In our system, we were able to select for minimal sequence changes that have potent biological effects. These observations have implications in alternative splicing mechanisms, where weak splice sites may play a role. Our results suggest that minor differences in composition can result in a significantly weakened polypyrimidine tract.

In general, there is a positive correlation between the functional strength and the length of polypyrimidine tracts (29, 36, 38). Also, uridine stretches within the polypyrimidine tract are important for the activity of short tracts (38). In our study, a U-to-C substitution of an isolated uridine residue, U(−15)C, produced a significant reduction in splicing efficiency. The second suppressor, U(−9)C, affects a uridine stretch and further reduces splicing efficiency in the presence of the U(−15)C mutation. A similar U-to-C suppressor mutation within a uridine stretch was described by Chen and Chasin (6).

Our results may reflect on the general mechanism of 3′ splice site selection. One model suggests that the 3′ splice site is selected by scanning from the branch point-polypyrimidine tract to the next downstream AG (42). In a simple scanning model, the sequences between these two elements do not play a direct role. Results from the other studies (31, 36) argue against a simple scanning model. Here, we have shown that sequences between the branch point and the 3′ splice site can influence the efficiency of the second step of splicing, suggesting that selection of the 3′ splice site in the second step is not the result of simple scanning.

The mechanism(s) of the U-to-C suppressor mutations in the polypyrimidine tract remains to be investigated. However, it seems likely that they affect the binding of protein splicing factors or complexes. Several studies indicate that major base-pairing shifts take place within the spliceosome during the transition between the first and second steps (see references 28, 30, and 43 for recent reviews). In the second step, the newly formed 3′-OH of exon 1 must be directed to the phosphate at the 3′ splice junction; the U5 snRNP appears to provide a "guide sequence" for this step. Protein factors are likely to be important in these steps to mediate the dynamic changes in base pairing and for stabilization of limited base pairing between U snRNAs and the pre-mRNA substrate. In higher eukaryotes, several proteins are believed to interact with the polypyrimidine tract, including U2AF (49), PTB (polypyrimidine tract-binding protein) (11, 12, 32), PSF (PTB-associated splicing factor) (33), and the intron-binding protein (IBP) (46). The observation that the polypyrimidine tract binds a number of factors, combined with a specific role for the polypyrimidine tract in the second step, suggests that different factors may bind sequentially during each step.

There are several examples of *cis* mutations or modifications that specifically affect the second step of splicing. These can be exploited to trap intermediate complexes for compositional analysis. One such study has revealed that PSF is essential for the second step (13). Our preliminary UV cross-linking experiments (3a) indicate differential binding of several protein factors when we compare the various mutants described here. One advantage of our system is that the mutations were biologically selected to produce suboptimal splicing. These mutations are distinct from the more severe defects produced by site-directed mutagenesis and may reveal more subtle mechanisms of regulation involving altered affinities for splicing factors.

What is the biological significance of the second-step blocks observed in vitro? Here, we show that viruses containing the IS1, IS1gg, IS1cuU(−15)C, and IS1cuU(−9,−15)C mutations also accumulate significant levels of lariat-exon 2 in vivo. In contrast, no lariat-exon 2 could be detected in cells infected with wild-type virus. The selection in this system is presumably for sufficient levels of the cytoplasmic form of unspliced viral RNA. It is unclear how a block in the second step would allow maintenance of unspliced RNA. We cannot rule out the possibility that the suppressor mutations have some effect on the first step and the effects on the second step are irrelevant. However, detection of splicing intermediates in vivo is rare, and this observation itself suggests that the intermediates do play a role in regulation. The fact that we have independently isolated two distinct second-step suppressor mutations, IS1 and IS1cuU(−15)C, further supports this suggestion. We have considered at least three possible models whereby the accumulation of intermediates in vivo might be related to the regulation we have observed. In model A, step 2 is simply rate limiting, as opposed to step 1 being rate limiting for wild-type virus. In model B, stalling after step 1 may allow an unusual reverse reaction that regenerates unspliced RNA. In model C, the intermediates themselves play a direct role in regulation. If we assume that the selection is for preservation of unspliced RNA, model A does not seem valid since the completion of step 1 would destroy the unspliced RNA. On the contrary, the results of numerous experiments indicate that wild-type levels of unspliced RNA are associated with these suppressor mutations. Although model B cannot be formally excluded, it seems unlikely. We currently favor model C, which suggests an active role for intermediates in regulation. One possible mechanism for this regulation is that stalled intermediates interfere with new rounds of splicing, at an early step. This would require that one or more splicing factors are limiting in vivo and that the stalled intermediates act to sequester these factors and prevent them from recycling.

In summary, our findings clearly demonstrate that the efficiency of the second step of splicing can be influenced by the polypyrimidine tract and that subtle U-to-C transitions can have a potent effect. Also, our results suggest a model in which stalled intermediates play a role in splicing regulation. Study of the biochemical basis of these effects may provide further insights into the mechanism of RNA splicing.

ACKNOWLEDGMENTS

We thank David Lazinski and Kevin Ryder for critical reading of the manuscript. We also acknowledge the contribution of Kim Scatta, who constructed pSP73ASV. We thank Marie Estes for excellent assistance in preparation of the manuscript. We also acknowledge the DNA Synthesis Facility of Fox Chase Cancer Center for providing oligodeoxynucleotides.

Support for this work was provided by National Institutes of Health grants CA-47486 and CA-06927, a grant from the Pew Charitable Trust, a grant for infectious disease research from Bristol-Myers Squibb Foundation, and also by an appropriation from the Commonwealth of Pennsylvania. X.-D. Fu is a Searle Scholar and is also supported by grants from the Cancer Research Coordination Committee of the University of California and from the National Institutes of Health.

REFERENCES

1. **Arrigo, S., and K. Beemon.** 1988. Regulation of Rous sarcoma virus RNA splicing and stability. Mol. Cell. Biol. **8:**4858–4867.
2. **Ausubel, F. M., R. Brent, R. E. Kingston, D. D. Moore, J. G. Seidman, J. A. Smith, and K. Struhl (ed.).** 1992. Short protocols in molecular biology, 2nd ed. Greene Publishing Assoc. and John Wiley and Sons, Inc., New York.
3. **Borroto-Esoda, K., and L. R. Boone.** 1994. Development of a human immunodeficiency virus-1 in vitro DNA synthesis system to study reverse transcriptase inhibitors. Antivir. Res. **23:**235–249.

3a. **Bouck, J.** Unpublished data.

4. **Bray, M., S. Prasad, J. W. DuBay, E. Hunter, K.-T. Jeang, D. Rekosh, and**

M.-L. Hammarskjöld. 1994. A small element from the Mason-Pfizer monkey virus genome makes human immunodeficiency virus type 1 expression and replication Rev-independent. Proc. Natl. Acad. Sci. USA **91:**1256–1260.
5. **Chang, D. D., and P. A. Sharp.** 1990. Messenger RNA transport and HIV *rev* regulation. Science **249:**614–615.
6. **Chen, I.-T., and L. A. Chasin.** 1993. Direct selection for mutations affecting specific splice sites in a hamster dihydrofolate reductase minigene. Mol. Cell. Biol. **13:**289–300.
7. **Coffin, J. M.** 1990. Retroviridae and their replication, p. 1437–1500. *In* B. N. Fields and D. M. Knipe (ed.), Fields' virology. Raven Press, New York.
8. **Dominski, Z., and R. Kole.** 1991. Selection of splice sites in pre-mRNAs with short internal exons. Mol. Cell. Biol. **11:**6075–6083.
9. **Fu, X.-D., R. A. Katz, A. M. Skalka, and T. Maniatis.** 1991. The role of branchpoint and 3′-exon sequences in the control of balanced splicing of avian retrovirus RNA. Genes Dev. **5:**211–220.
10. **Fu, X.-Y., H. Ge, and J. L. Manley.** 1988. The role of the polypyrimidine stretch at the SV40 early pre-mRNA 3′ splice site in alternative splicing. EMBO J. **7:**809–817.
11. **Garcia-Blanco, M. A., S. F. Jamison, and P. A. Sharp.** 1989. Identification and purification of a 62,000-dalton protein that binds specifically to the polypyrimidine tract of introns. Genes Dev. **3:**1874–1886.
12. **Gil, A., P. A. Sharp, S. F. Jamison, and M. Garcia-Blanco.** 1991. Characterization of cDNA's encoding the polypyrimidine tract-binding protein. Genes Dev. **5:**1224–1236.
13. **Gozani, O., J. G. Patton, and R. Reed.** 1994. A novel set of spliceosome-associated proteins and the essential splicing factor PSF bind stably to pre-mRNA prior to catalytic step II of the splicing reaction. EMBO J. **13:**3356–3367.
14. **Green, M. R.** 1991. Biochemical mechanisms of constitutive and regulated pre-mRNA splicing. Annu. Rev. Cell Biol. **7:**559–599.
15. **Hodges, D., and S. I. Bernstein.** 1994. Genetic and biochemical analysis of alternative RNA splicing. Adv. Genet. **31:**207–281.
16. **Katz, R. A., X.-D. Fu, A. M. Skalka, and J. Leis.** 1986. Avian retrovirus nucleocapsid protein, pp12, produced in *Escherichia coli* has biochemical properties identical to unphosphorylated viral proteins. Gene **50:**361–369.
17. **Katz, R. A., M. Kotler, and A. M. Skalka.** 1988. *cis*-acting intron mutations that affect the efficiency of avian retroviral RNA splicing: implication for mechanisms of control. J. Virol. **62:**2686–2695.
18. **Katz, R. A., and A. M. Skalka.** 1990. Generation of diversity in retroviruses. Annu. Rev. Genet. **24:**409–445.
19. **Katz, R. A., and A. M. Skalka.** 1990. Control of retroviral RNA splicing through maintenance of suboptimal processing signals. Mol. Cell. Biol. **10:**696–704.
20. **Kjems, J., and P. A. Sharp.** 1993. The basic domain of Rev from human immunodeficiency virus type 1 specifically blocks the entry of U4/U6-U5 small nuclear ribonucleoprotein in spliceosome assembly. J. Virol. **67:**4769–4776.
21. **Lee, C.-G., P. D. Zamore, M. R. Green, and J. Hurwitz.** 1993. RNA annealing activity is intrinsically associated with U2AF. J. Biol. Chem. **268:**13472–13478.
22. **Lu, X., J. Heimer, D. Rekosh, and M.-L. Hammarskjöld.** 1990. U1 small nuclear RNA plays a direct role in the formation of a rev-regulated human immunodeficiency virus env mRNA that remains unspliced. Proc. Natl. Acad. Sci. USA **87:**7598–7602.
23. **Maniatis, T.** 1991. Mechanisms of alternative pre-mRNA splicing. Science **251:**33–34.
24. **Mattox, W., L. Ryner, and B. S. Baker.** 1992. Autoregulation and multifunctionality among trans-acting factors that regulate alternative pre-mRNA processing. J. Biol. Chem. **267:**19023–19026.
25. **McKeown, M.** 1992. Alternative mRNA splicing. Annu. Rev. Cell Biol. **8:**133–155.
26. **McNally, M. T., and K. Beemon.** 1992. Intronic sequences and 3′ splice sites control Rous sarcoma virus RNA splicing. J. Virol. **66:**6–11.
27. **McNally, M. T., R. R. Gontarek, and K. Beemon.** 1991. Characterization of Rous sarcoma virus intronic sequences that negatively regulate splicing. Virology **185:**99–108.
28. **Moore, M. J., C. C. Query, and P. A. Sharp.** 1993. Splicing of precursors to messenger RNAs by the spliceosome, p. 303–357. *In* R. Gesteland and J. Atkins (ed.), The RNA world. Cold Spring Harbor Press, Cold Spring Harbor, N.Y.
29. **Mullen, M. P., C. W. J. Smith, J. G. Patton, and B. Nadal-Ginard.** 1991. α-Tropomyosin mutually exclusive exon selection: competition between branchpoint/polypyrimidine tracts determines default exon choice. Genes Dev. **5:**642–655.
30. **Nilsen, T. W.** 1994. RNA-RNA interactions in the spliceosome: unraveling the ties that bind. Cell **78:**1–4.
31. **Patterson, B., and C. Guthrie.** 1991. A U-rich tract enhances usage of an alternative 3′ splice site in yeast. Cell **64:**181–187.
32. **Patton, J. G., S. A. Mayer, P. Tempst, and B. Nadal-Ginard.** 1991. Characterization and molecular cloning of polypyrimidine tract-binding protein: a component of a complex necessary for pre-mRNA splicing. Genes Dev. **5:**1237–1251.
33. **Patton, J. G., E. B. Porro, J. Galceran, P. Tempst, and B. Nadal-Ginard.** 1993. Cloning and characterization of PSF, a novel pre-mRNA splicing factor. Genes Dev. **7:**393–406.
34. **Qian, L., M. N. Vu, M. S. Carter, J. Doskow, and M. F. Wilkinson.** 1993. T cell receptor-β mRNA splicing during thymic maturation in vivo and in an inducible T cell clone in vitro. J. Immunol. **151:**6801–6814.
35. **Query, C. C., M. J. Moore, and P. A. Sharp.** 1994. Branch nucleophile selection in pre-mRNA splicing: evidence for the bulged duplex model. Genes Dev. **8:**587–597.
36. **Reed, R.** 1989. The organization of 3′ splice-site sequences in mammalian introns. Genes Dev. **3:**2113–2123.
37. **Rio, D. C.** 1992. RNA processing. Curr. Opin. Cell Biol. **4:**444–452.
38. **Roscigno, R. F., M. Weiner, and M. A. Garcia-Blanco.** 1993. A mutational analysis of the polypyrimidine tract of introns. J. Biol. Chem. **268:**11222–11229.
39. **Schwartz, D. E., R. Tizard, and W. Gilbert.** 1983. Nucleotide sequence of Rous sarcoma virus. Cell **32:**853–869.
40. **Smith, C. W. J., and B. Nadal-Ginard.** 1989. Mutually exclusive splicing of α-tropomyosin exons enforced by an unusual lariat branch point location; implications for constitutive splicing. Cell **56:**749–758.
41. **Smith, C. W. J., J. G. Patton, and B. Nadal-Ginard.** 1989. Alternative splicing in the control of gene expression. Annu. Rev. Genet. **23:**527–577.
42. **Smith, C. W. J., E. B. Porro, J. G. Patton, and B. Nadal-Ginard.** 1989. Scanning from an independently specified branch point defines the 3′ splice site of mammalian introns. Nature (London) **342:**243–247.
43. **Steitz, J. A.** 1992. Splicing takes a holiday. Science **257:**888–889.
44. **Stoltzfus, C. M., and S. J. Fogarty.** 1989. Multiple regions in the Rous sarcoma virus *src* gene intron act in *cis* to affect the accumulation of unspliced RNA. J. Virol. **63:**1669–1676.
45. **Tanaka, K., A. Watakabe, and Y. Shimura.** 1994. Polypurine sequences within a downstream exon function as a splicing enhancer. Mol. Cell. Biol. **14:**1347–1354.
46. **Tazi, J., C. Alibert, J. Temsamani, I. Reveillaud, G. Cathala, C. Brunel, and P. Jeanteur.** 1986. A protein that specifically recognizes the 3′ splice site of mammalian pre-mRNA introns is associated with a small nuclear ribonucleoprotein. Cell **47:**755–766.
47. **Wu, J., and J. L. Manley.** 1989. Mammalian pre-mRNA branch site selection by U2 snRNP involves base pairing. Genes Dev. **3:**1553–1561.
48. **Xu, R., J. Teng, and T. A. Cooper.** 1993. The cardiac troponin T alternative exon contains a novel purine-rich positive splicing element. Mol. Cell. Biol. **13:**3660–3674.
49. **Zamore, P. D., and M. R. Green.** 1989. Identification, purification, and biochemical characterization of U2 small nuclear ribonucleoprotein auxiliary factor. Proc. Natl. Acad. Sci. USA **86:**9243–9247.
50. **Zhuang, Y., A. M. Goldstein, and A. M. Weiner.** 1989. UACUAAC is the preferred branch site for mammalian mRNA splicing. Proc. Natl. Acad. Sci. USA **86:**2752–2756.
51. **Zhuang, Y., and A. M. Weiner.** 1989. A compensatory base change in human U2 snRNA can suppress a branch site mutation. Genes Dev. **3:**1545–1552.